Design considerations for low-light level low-Fresnel number optical systems

Christoph Baranec

Caltech Optical Observatories, California Institute of Technology, 1200 East California Boulevard, Pasadena, California 91125, USA;
baranec@astro.caltech.edu

Received 3 September 2009; accepted 7 October 2009;
posted 9 October 2009 (Doc. ID 116365); published 4 November 2009

Low-Fresnel number optical systems exhibit significant diffraction effects that cause a shift in the peaks of on-axis irradiance away from the geometric focal point. This is currently interpreted as a change of the focal length of an optical system, leading optical system designers to compensate for the effect by assuming the image plane is coincident with the peak of on-axis irradiance. While this may be an appropriate interpretation for certain applications, I show that despite the shift in peak irradiance away from the geometrical focal point, a change in a system's optical power will not increase the on-axis irradiance at that distance. This is important for low-light level applications where it is necessary to mitigate diffraction induced transmission losses. I also show that low-Fresnel number systems have increased tolerance on system power at the geometrical focal point and as a result are inherently achromatic.

OCIS codes: 050.1940, 080.2468, 350.3950.

1. Introduction

The degree of an optical system's nongeometric nature can be determined by calculating its Fresnel number. As a system's Fresnel number drops below ~10, diffraction increasingly affects optical propagation. For a simple optical system comprised of a coincident thin lens and circular aperture with an object located at infinity, the Fresnel number, FN, can be expressed as

$$\mathrm{FN} = \phi a^2/\lambda, \tag{1}$$

where a is the radius of the aperture and ϕ is the optical power of the lens. Sheppard and Törörk [1] suggested a modified version of Eq. (1) that does not assume the system $F/\#$ is large. However, in practical macroscopic optical systems where $a \gg \lambda$, values of $F/\#$ for low-Fresnel number systems are typically quite large, $F/\# \gg 1$; thus Eq. (1) is a reasonable approximation.

Particularly relevant topical examples of low-Fresnel number systems are the extreme contrast adaptive optics systems used to support direct imaging of exoplanets. The wave front sensors for these systems will operate at over 2 kHz with subapertures as small as ~8 cm, having Fresnel numbers as low as 0.6 at $\lambda = 700$ nm [2–4]. Additionally, the high-cost sodium D_2 line excitation lasers used in astronomy require projection systems with Fresnel numbers ~1 [5,6]. Both applications are examples of low-light level optical systems that are extremely sensitive to transmission losses, including those caused by diffraction, and should be properly designed to make the best use of the available photons.

As the Fresnel number of an optical system decreases, the location of peak on-axis irradiance, Z_p, shifts away from the geometric focal point, and for a positive lens, this shift is toward a system's exit pupil. Examples of the shift can be seen in Fig. 1, where the normalized on-axis irradiance profiles for four different optical systems are presented, with z representing the distance from the exit pupil. For each of the different Fresnel number systems, 100, 10, 1, and

0003-6935/09/326259-05$15.00/0

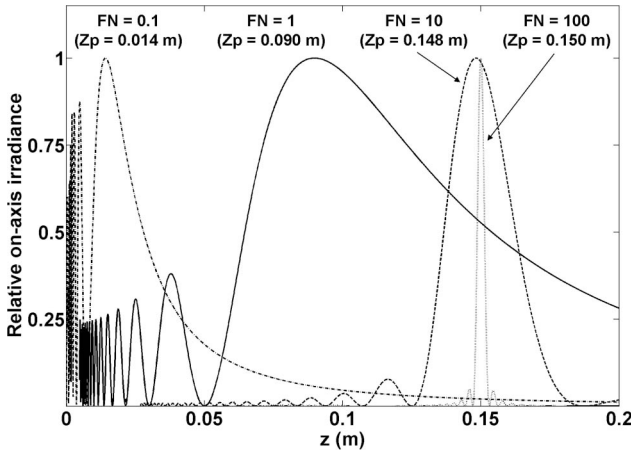

Fig. 1. Examples of the shift in Z_p away from the geometrical focal distance of 0.15 m for optical systems of different Fresnel number, normalized to peak irradiance. All systems assume a uniformly illuminated circular aperture of diameter 600 μm with a thin lens, $\phi = 6.67\,\mathrm{m}^{-1}$. Different Fresnel numbers are achieved by varying λ from 6 nm to 6 μm.

0.1, the ratio of Z_p to the geometric focal length, $1/\phi$, is 1.000, 0.988, 0.598, and 0.095 respectively.

The three-dimensional irradiance distributions behind simple optical systems consisting of a coincident thin lens and aperture have been studied extensively, and theoretical derivations of Z_p have been calculated (e.g., [7–13]). In these previous studies, the shift of Z_p away from the geometric focal point has been identified as a change in an optical system's effective focal length. This interpretation of Z_p may be misleading, as I will show here that Z_p does not necessarily coincide with the point of maximum irradiance at a desired observation distance.

2. Complex Amplitude and Irradiance Behind a Lens

The equation for the complex amplitude U for the geometry shown in Fig. 2 at a point P_0 behind an open aperture Σ at P_1 is given by [14], Eq. 3–26,

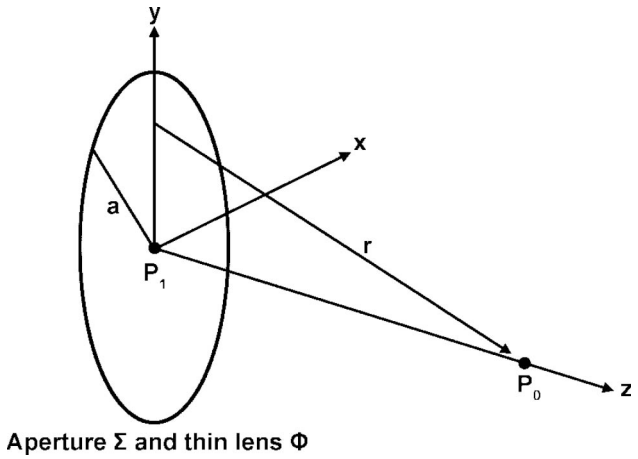

Fig. 2. Geometry of a coincident aperture Σ of radius a and a thin lens of power ϕ at P_1.

$$U(P_0) = \frac{1}{j\lambda}\int\int_{\Sigma} U(P_1)\frac{\exp\left[\frac{2\pi j}{\lambda}r\right]}{r}\cos[r]\mathrm{d}s, \qquad (2)$$

where $U(P_1)$ can be expressed as

$$U(P_1) = A\,\exp\left[\frac{2\pi j}{\lambda}\frac{\phi(z^2 - r^2)}{2}\right] \qquad (3)$$

for a source at infinity incident on a thin paraxial lens of power ϕ at P_1. Substituting Eq. (3) into Eq. (2) and integrating over r, the expression for the on-axis complex amplitude at P_0 can be written as

$$U(z) = \frac{A}{j\lambda}\int_{z}^{\sqrt{z^2+a^2}} \exp\left[\frac{2\pi j}{\lambda}\left(r + \frac{\phi}{2}(z^2 - r^2)\right)\right]\frac{\cos[r]}{r}\mathrm{d}r. \qquad (4)$$

Figure 3 shows the on-axis irradiance, $I(z) = |U(z)|^2$, profiles behind a uniformly illuminated system with a 600 μm circular aperture and coincident thin lenses of different optical powers. Irradiance is maximized at an example observation distance of $z = 0.15$ m by using a lens with $\phi = 6.67\,\mathrm{m}^{-1} = (0.15\,\mathrm{m})^{-1}$ (FN = 0.94; $F/\# = 250$). Note that for this lens, $Z_p = 0.087$ m, and for a lens with no power, $Z_p = 0.142$ m.

This can be explained from Eq. (4) to within the paraxial approximation; a spherical lens of $\phi = z^{-1}$ exactly compensates for the path length difference between the on-axis point at the geometric focal distance and every point on the aperture. All of the phasors are lined up in the same direction, and upon integration, calculated irradiance is at a maximum. For any other lens, the phasors will not all be lined up, causing partial destructive interference and a loss of irradiance.

The irradiance distribution behind an optical system in the $x-y$ plane at point P_0 can be calculated numerically point-by-point with an appropriate change in limits of integration and represents the point spread function (PSF) of the optical system. By examining the PSF's full width at half-maximum (FWHM) in combination with the on-axis irradiance at the observation distance, the relative encircled energy within a canonical $\lambda F/\# = \lambda z/(2a)$ diameter for different powers of lenses can be evaluated. For the optical system presented in Fig. 3 ($\lambda F/\# = 158.8\mu$m), it was found that the FWHM of the PSF is minimized at 163.1 μm when $\phi = 6.67\,\mathrm{m}^{-1}$ and only changes very slowly, with the FWHM expanding to 168.7 μm for lenses of no power and double the power—both having on-axis irradiances at $z = 0.15$ m that are 45% of the $\phi = 6.67\,\mathrm{m}^{-1}$ lens. Since the FWHM of the PSF changes by relatively small amounts, the encircled energy within $\lambda F/\#$ is therefore proportional to the on-axis intensity and is

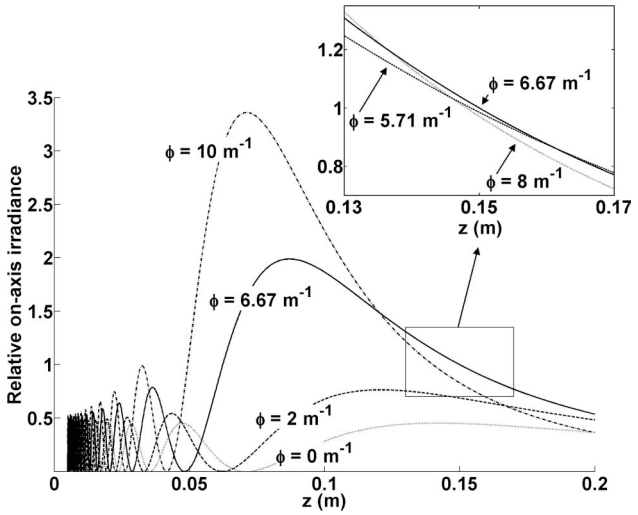

Fig. 3. Relative on-axis irradiance as a function of distance from the exit pupil of a uniformly illuminated ($\lambda = 635$ nm) system with a 600 μm circular aperture and various optical power lenses. A magnification of the area around $z = 0.15$ m is shown (upper right).

maximized when a lens has optical power equal to the inverse of the observation distance.

3. Measurement of Irradiance Behind a Lens

I have experimentally verified the on-axis irradiance for the system presented in Fig. 3 at the point $z = 0.15$ m with lenses of a range of optical powers. Figure 4 shows the optical layout of the experimental setup. A 600 μm circular pinhole aperture was illuminated with collimated light from a power stabilized laser source. A beam splitter and a photodiode were used to confirm the stability of the source irradiance. Uncoated spherical plano-convex lenses of various optical powers were placed in the beam such that the collimated light was incident on the planar side

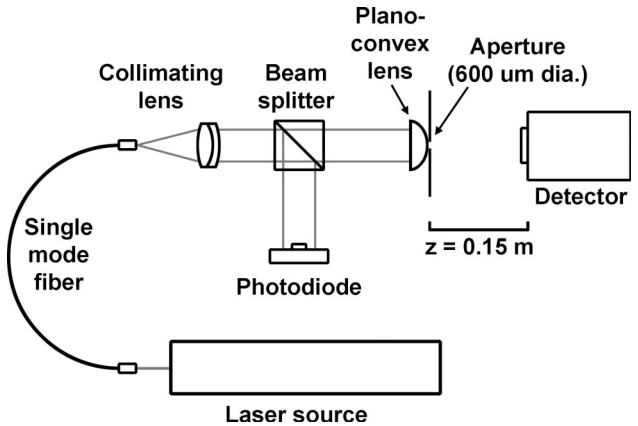

Fig. 4. Experimental setup to measure the on-axis irradiance at $z = 0.15$ m as a function of lens optical power. The $\lambda = 635$ nm laser is coupled to a single mode fiber, and the diverging output is collimated by an achromatic lens. The stability of irradiance of the collimated beam is measured with a beam splitter and overfilled photodiode detector. The collimated light is incident on the planar side of a plano-convex lens with the convex side in contact with the 600 μm diameter circular aperture. A CMOS detector is then placed 0.15 m away from the aperture.

with the convex side in contact with the aperture. This lens configuration avoids condensation of light before the aperture, and for the shortest focal length lens, there is a negligible, $\sim 10^{-4}$ wave, amount of added spherical aberration. An 8 bit complementary metal-oxide semiconductor (CMOS) detector (PixeLink PL-B781F) with 3.5 μm pixels observed the two-dimensional irradiance distribution at $z = 0.15$ m. The detector was configured to give a linear response with respect to intensity, and the analog-to-digital converter dominated the measurement and shot noise. Figure 5 shows the theoretical and measured on-axis irradiance at this distance as a function of inverse power for different lenses. Deviations of the measured points from the theoretical curve are likely due to systematic errors (e.g., nonperfect collimation or manufacturing errors in aperture size.) The on-axis irradiance at $z = 0.15$ m is found to be maximized when $\phi = 6.67\ \mathrm{m}^{-1} = (0.15\ \mathrm{m})^{-1}$.

4. Design Implications

For low-light level low-Fresnel systems where mitigation of diffraction losses is important, it is therefore important to consider placing a detector at the geometrical focus of an optical system to maximize the amount of light on the detector. This result was also found by Carter [15] for propagating Gaussian beams. He found that a laser communications telescope (FN ~ 0.08) transmits the maximum possible intensity to a receiver when designed such that the geometrical focus is placed at the receiver. Carter, however, was more interested in mitigating the detrimental effects of having Z_p close to the transmitting telescope (e.g., thermal blooming and other nonlinear effects) than actually maximizing transmission to the receiver and therefore suggested a "focal shift correction in systems design" to instead adjust the optical power of the transmitting telescope such that Z_p occurred at the receiver. Even though

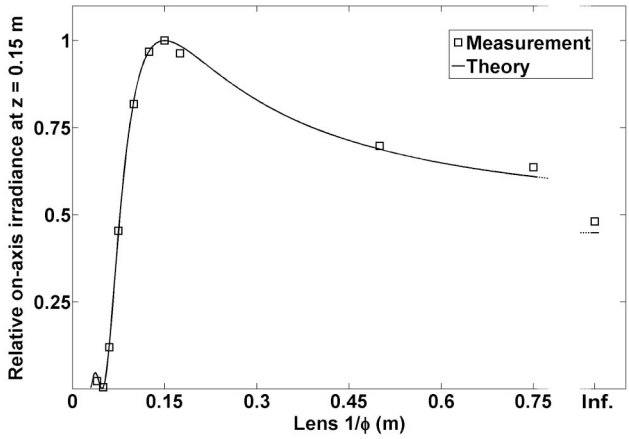

Fig. 5. Relative on-axis irradiance at $z = 0.15$ m for an optical system comprised of a uniformly illuminated ($\lambda = 635$ nm) 600 μm diameter circular aperture with various optical power lenses ($1/\phi$ shown). The measured data are precise to ± 0.002 in relative irradiance as scaled here and to within $\pm 1\%$ of $1/\phi$.

there was diminished intensity at the receiver, this precluded any higher irradiance before the receiver.

Choosing to place a detector in an optical system at Z_p, and not at the geometrical focus, has been used by Ruffieux *et al.* [16] to claim that microlens systems of low-Fresnel number, such as Shack–Hartmann wavefront sensors, can be designed to be achromatic with a single lens material. Ruffieux *et al.* show how the change in effective lens power at different wavelengths introduced by the wavelength dependent index of refraction of the lens material can be offset by the change in Z_p as a function of wavelength. While this does not cause the location of Z_p to change with wavelength, there is a loss of over 50% in on-axis irradiance for a FN ~ 1 optical system by placing a detector at Z_p instead of adjusting the power of an optical system such that the geometrical focus is located at the detector. The consequences of this design choice should be considered carefully for low-light level systems, as the apparent benefit may be offset by severe irradiance losses.

Additionally, the perceived chromatic errors of low-Fresnel number optical systems cited by Ruffieux *et al.* have been overstated. Figure 6 shows the on-axis irradiance at $z = 0.15$ m as a function of lens power for the different Fresnel number systems described in Fig. 1. For a decrease in irradiance of 5% for the FN $= 100$ system, $1/\phi$ can change by at most $\pm 0.27\%$. However, for the systems of FN $= 10$, 1, and 0.1, the tolerance on $1/\phi$ is increased to $\pm 2.5\%$, -20 to $+33\%$, and -71% to no power, respectively, for the same loss of irradiance. Not only does the tolerance on optical power for low-Fresnel number optical systems alleviate manufacturing tolerances on the radius of curvature of optical surfaces, but it also translates to increased achromatic properties. At the observation distance, the change in lens material index of refraction as a function of wavelength can be interpreted as a wavelength dependent error in lens power. For the interface between a glass lens and air,

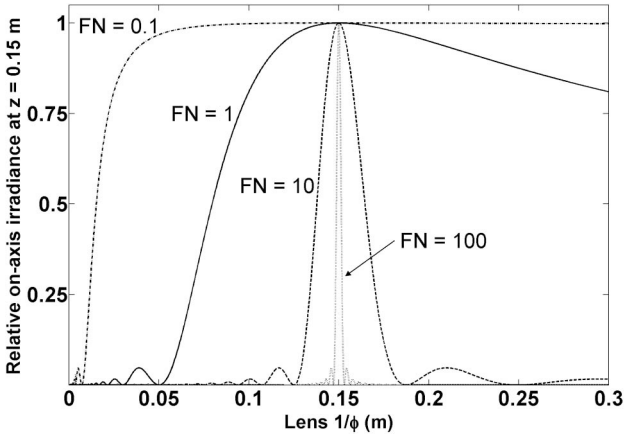

Fig. 6. Relative on-axis irradiance at $z = 0.15$ m as a function of optical power for the different Fresnel number systems presented in Fig. 1.

$$\Delta(1/\phi) = \mathrm{RoC}\frac{\Delta n}{(n-1)^2}, \tag{5}$$

where RoC is the radius of curvature of the lens surface. As the Fresnel number decreases, the tolerance on optical power increases and the irradiance losses over the operating wavelength bandwidth decrease. For example, at the interface between air and a lens made of N-BK7 ($n_d = 1.51680$ and $n_F - n_C = 0.008054$) with a geometrical focal distance of 0.15 m, $\Delta(1/\phi) = \pm 0.8\%$ over $\lambda = 486$ to 686 nm. For a FN $=$ 100 optical system, there would be an irradiance loss of $\sim 57\%$ at each end of the wavelength range. However, for a FN $= 1$ optical system, there would only be an irradiance decrease of $<0.01\%$ at each end of the wavelength range. Therefore there is little need to correct for chromatic effects in low-Fresnel number optical systems.

5. Conclusion

It has been shown that despite the shift in peak irradiance away from the geometrical focal point for low-Fresnel number optical systems, on-axis irradiance at an observation distance is maximized by designing a system such that the geometrical focal point is coincident with the observation distance. The FWHM of the PSF at this point changes very weakly with a change in optical system power, and therefore encircled energy within a canonical $\lambda F/\#$ diameter is also maximized when the on-axis irradiance is maximized. This is an important consideration when designing low-light level low-Fresnel number systems that are sensitive to diffraction induced transmission losses. Additionally, all low-Fresnel number optical systems benefit from an increased tolerance on optical system power at the geometrical focus, which both eases manufacturing tolerances on the radius of curvature of optical surfaces and makes the systems inherently achromatic.

This work has been supported by the National Science Foundation (NSF) under grant AST-0619922.

References

1. C. J. R. Sheppard and P. Törörk, "Dependence of focal shift on Fresnel number and angular aperture," Opt. Lett. **23**, 1803–1804 (1998).
2. T. Fusco, G. Rousset, J.-F. Sauvage, C. Petit, J.-L. Beuzit, K. Dohlen, D. Mouillet, J. Charton, M. Nicolle, M. Kasper, P. Baudoz, and P. Puget, "High-order adaptive optics requirements for direct detection of extrasolar planets: application to the SPHERE instrument," Opt. Express **14**, 7515–7534 (2006).
3. R. Dekany, A. Bouchez, M. Britton, V. Velur, M. Troy, J. C. Shelton, and J. Roberts, "PALM-3000: visible-light AO on the 5.1-meter Telescope," Proc. SPIE **6272**, 62720G (2006).
4. C. Baranec, "High-order wavefront sensing system for PALM-3000," Proc. SPIE **7015**, 70155M (2008).
5. M. van Dam, A. Bouchez, D. Mignant, E. Johansson, P. Wizinowich, R. Campbell, J. Chin, S. Hartman, R. Lafon, P. Stomski, and D. Summers, "The W. M. Keck observatory laser guide star adaptive optics system: performance characterization," Publ. Astron. Soc. Pac. **118**, 310–318 (2006).

6. V. Velur, E. Kibblewhite, R. Dekany, M. Troy, H. Petrie, R. Thicksten, G. Brack, T. Trin, and M. Cheselka, "Implementation of the Chicago sum frequency laser at Palomar laser guide star test bed," Proc. SPIE **5490**, 1033–1040 (2004).
7. H. Osterberg and L. W. Smith, "Closed solutions of Rayleighs diffraction integral for axial points," J. Opt. Soc. Am. **51**, 1050–1054 (1961).
8. Y. Li, "Three-dimensional intensity distribution in low-Fresnel-number focusing systems," J. Opt. Soc. Am. A **4**, 1349–1353 (1987).
9. M. Martínez-Corral, C. J. Zapata-Rodríguez, P. Andrés, and E. Silvestre, "Effective Fresnel-number concept for evaluating the relative focal shift in focused beams," J. Opt. Soc. Am. A **15**, 449–455 (1998).
10. Y. Li, "Focal shifts in diffracted converging electromagnetic waves. II. Rayleigh theory," J. Opt. Soc. Am. A **22**, 77–83 (2005).
11. Y. Li, "Focal shift in small-Fresnel-number focusing systems of different relative aperture," J. Opt. Soc. Am. A **20**, 234–239 (2003).
12. Y. Zhong, "Focal shift in focused truncated pulsed-laser beam," Appl. Opt. **46**, 6454–6459 (2007).
13. R. Borghi, M. Santarsiero, and S. Vicalvi, "Focal shift of focused flat-topped beams," Opt. Commun. **154**, 243–248 (1998).
14. J. W. Goodman, *Introduction to Fourier Optics* (McGraw-Hill, 1968).
15. W. Carter, "Focal shift and concept of effective Fresnel number for a Gaussian laser beam," Appl. Opt. **21**, 1989–1994 (1982).
16. P. Ruffieux, T. Scharf, H. P. Herzig, R. Völkel, and K. J. Weible, "On the chromatic aberration of microlenses," Opt. Express **14**, 4687–4694 (2006).